

# TokenTrace: Multi-Concept Attribution through Watermarked Token Recovery

Li Zhang  
University of California, San Diego  
liz042@ucsd.edu

Shruti Agarwal  
Adobe

John Collomosse  
Adobe

Pengtao Xie  
University of California, San Diego

Vishal Asnani  
Adobe

## Abstract

*Generative AI models pose a significant challenge to intellectual property (IP), as they can replicate unique artistic styles and concepts without attribution. While watermarking offers a potential solution, existing methods often fail in complex scenarios where multiple concepts (e.g., an object and an artistic style) are composed within a single image. These methods struggle to disentangle and attribute each concept individually. In this work, we introduce TokenTrace, a novel proactive watermarking framework for robust, multi-concept attribution. Our method embeds secret signatures into the semantic domain by simultaneously perturbing the text prompt embedding and the initial latent noise that guide the diffusion model’s generation process. For retrieval, we propose a query-based TokenTrace module that takes the generated image and a textual query specifying which concepts need to be retrieved (e.g., a specific object or style) as inputs. This query-based mechanism allows the module to disentangle and independently verify the presence of multiple concepts from a single generated image. Extensive experiments show that our method achieves state-of-the-art performance on both single-concept (object and style) and multi-concept attribution tasks, significantly outperforming existing baselines while maintaining high visual quality and robustness to common transformations.*

## 1. Introduction

Text-to-image foundation models [4, 21, 31], propelled by large-scale diffusion architectures [11, 30], have demonstrated unprecedented success in generating high-fidelity, complex visual content from natural language descriptions. This progress has brought generative AI to the forefront of creative industries [19]. However, this power introduces a critical challenge in proactive attribution: the need to embed imperceptible, robust watermarks into generated content to

verify ownership and trace provenance [13, 55]. This task is fundamental to protecting the intellectual property of artists and creators whose unique styles and concepts are used to train these models. Recent state-of-the-art methods, such as ProMark [2], have pioneered a “proactive” approach, embedding imperceptible watermarks directly into the pixel space of images. These methods train the diffusion model to preserve these spatial watermarks, allowing a decoder to later detect them in generated images and establish a causal connection to the original training examples that contribute to the generations. Such invention is effective for the general concept attribution task.

Despite progress in this area, existing watermarking methods face notable limitations. Approaches that operate in the pixel domain are often fragile, failing to survive common transformations like compression or cropping [2, 34, 55]. While more recent methods embedding watermarks into the latent space offer greater robustness [3, 29, 45], they fail to address a significant challenge posed by the compositional nature of generative AI. These models frequently generate images by combining multiple, distinct concepts (e.g., a specific character rendered in a unique artistic style). Existing attribution methods, which embed a single holistic watermark, are not designed for this scenario; they cannot disentangle and independently attribute multiple concepts when their visual representations overlap in the final image. This failure to attribute composed concepts is a major gap in protecting creator IP. While some recent works attempt multi-concept attribution [40], they struggle with signal interference and lack a precise mechanism for targeted retrieval.

In response to the above challenges, we introduce TokenTrace, a proactive watermarking framework for robust, multi-concept attribution. We hypothesize that a watermark’s robustness and specificity can be dramatically improved by associating it directly with the textual semantics of the concept it represents, a strategy inspired by the suc-

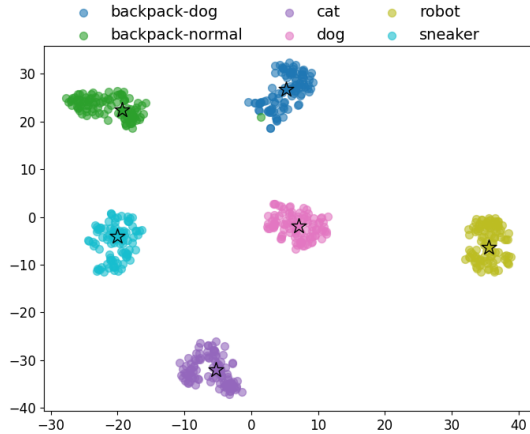


Figure 1. t-SNE visualization of predicted concept embeddings. The embeddings retrieved by TokenTrace module from DreamBooth-generated images (dots) form distinct, well-separated clusters around their ground-truth embeddings (stars), validating its ability to perform concept attribution.

cess of prompt-tuning in foundation models [20, 53]. This association is the key to solving the multi-concept challenge: instead of embedding competing signals into the limited pixel space, we link each concept’s secret to its unique representation within the text embedding. This approach fundamentally avoids the problem of spatial overlap, as the signatures are separated in the textual semantic domain before generation begins. TokenTrace achieves this via a novel dual-conditioning strategy. A concept’s secret is processed by two parallel networks: a concept encoder that perturbs the text prompt embedding and a secret mapper that perturbs the initial latent noise. By embedding the signature in both the semantic and latent domains, the watermark is deeply integrated into the generative process, ensuring both robustness and this crucial concept-level separation. To retrieve the watermark, we propose a query-based TokenTrace module designed to reverse this watermark encoding, which takes the watermarked image and a query prompt as inputs to predict the corresponding concept secrets. The feasibility of this retrieval approach was validated in a preliminary experiment<sup>1</sup>; as shown in a t-SNE visualization (Figure 9), TokenTrace module successfully maps generated images back to distinct, well-separated clusters for each concept.

Our work makes three key contributions:

- We propose TokenTrace, a novel framework that embeds watermarks into both the text prompt and latent noise domains, intrinsically tying the watermark to the concept’s semantics.
- We introduce a query-based module that can effectively disentangle and independently attribute multiple, overlapping concepts (such as objects and styles) from a single generated image.

<sup>1</sup>Detailed settings for this preliminary experiment can be found in the supplementary material.

- Our extensive experiments on both object and style concepts demonstrate that TokenTrace significantly outperforms state-of-the-art attribution baselines in both single-concept and multi-concept scenarios, all while maintaining high visual fidelity.

## 2. Related Works

**Generative Customization** The advent of large-scale text-to-image diffusion models has enabled remarkable image synthesis [30, 31, 33, 44, 48]. A significant and parallel line of research is generative customization, which focuses on personalizing these foundation models with novel, user-provided concepts [8, 22, 23, 46, 50]. Techniques such as Textual Inversion [14] and DreamBooth [31] allow models to learn a new concept from just a few example images, often by learning a new pseudo-token in the model’s text-embedding space or leaning a new set of model parameters for a customized concept. While this customization empowers creators to inject their unique intellectual property (IP) into the generative process, it also exposes that IP to misuse [9, 38, 39]. These learned concepts can be extracted and repurposed without permission, which introduces a critical need for robust attribution methods designed specifically for these personalized concepts.

**Watermarking and Concept Attribution for Generative Models** To address provenance and attribution, various watermarking techniques for generative models have been proposed [13, 18, 25, 45, 47], which are broadly categorized as passive or proactive. Passive watermarking applies a signature after generation [15, 35, 54]. This approach, while simple, adds computational cost, is easily defeated by common transformations, and is thus insufficient for reliable attribution. In contrast, proactive watermarking, our focus, integrates the signature during the generative process [2, 18, 41], making it inherently more robust to transformations and the necessary choice for causal attribution. Existing proactive methods embed signatures in the pixel-domain [2, 34] or latent-domain [3, 47]. However, these traditional methods typically embed a single, content-agnostic watermark, failing to link it to specific semantic concepts, which leads to the challenges we address next.

**Proactive Schemes** Proactive schemes embed signals into the generative process for tasks like deepfake detection [42, 52], manipulated content localization [1, 49], and concept attribution [2, 3]. While pixel-domain methods are fragile and fail when multiple concept spatially overlap, and latent-domain methods are robust but content-agnostic, a new category operates in the semantic domain [26], linking watermarks to textual representations. For instance, “Guarding Textual Inversion” [12] is designed for single-concept tracing and does not address compositional attribution. CustomMark [3] also customizes models via text

prompts for multi-concept attribution but struggles to disentangle concepts that are spatially overlapping. Thus, a robust, query-based mechanism for disentangling composed concepts remains a significant and unaddressed challenge.

### 3. Method

In this section, we present our method, TokenTrace, a proactive watermarking framework designed for robust, multi-concept attribution. As illustrated in Figure 2, our framework is composed of two primary stages: (a) a concept encoding stage that embeds concept secrets into the generative process, (b) a concept decoding stage that retrieves the corresponding concept secrets that indicated by a query prompt, and (c) the detailed architecture of our TokenTrace module.

#### 3.1. Concept Encoding

Our encoding process employs a novel dual-conditioning strategy that embeds a watermark by simultaneously perturbing the generative inputs in both the semantic domain (textual embeddings) and the latent domain (initial noise). As shown in Figure 2(a), this stage involves two parallel networks that process a concept secret ( $\mathcal{S}$ ):

- The concept encoder ( $f_{enc}$ ) targets the specific concept token to be watermarked. A user prompt embedding  $E_{prompt}$  is a collection of token embeddings  $\{e_1, \dots, e_c, \dots, e_k\}$ , where  $e_c$  is the target concept token embedding. The encoder  $f_{enc}$  takes the concept secret ( $\mathcal{S}$ ) and the corresponding concept token embedding ( $e_c$ ) as input to generate a perturbation. This perturbation is fused (via element-wise addition) only with the target token embedding  $e_c$  to create a perturbed token embedding  $\hat{e}_c$ . The final perturbed prompt embedding,  $\hat{E}_{prompt}$ , is calculated by replacing the original token:

$$\begin{cases} \hat{e}_c = e_c + f_{enc}(e_c, \mathcal{S}) \\ \hat{E}_{prompt} = \{e_1, \dots, \hat{e}_c, \dots, e_k\} \end{cases} \quad (1)$$

- The secret mapper ( $f_{map}$ ) takes only the concept secret ( $\mathcal{S}$ ) as input and generates a structured perturb gaussian pattern. This pattern is fused with the original noise pattern ( $z_T$ ) to create the perturbed initial noise,  $\hat{z}_T$ .

$$\hat{z}_T = z_T + f_{map}(\mathcal{S}) \quad (2)$$

Finally, the diffusion model ( $DM$ ) is conditioned on both of these inputs, the prompt embedding with perturbed concept token embeddings ( $\hat{E}_{prompt}$ ) and the perturbed noise ( $\hat{z}_T$ ), to generate the final watermarked image ( $I_{wm}$ ).

$$I_{wm} = DM(\hat{z}_T, \hat{E}_{prompt}) \quad (3)$$

By applying this dual-conditioning strategy, our method achieves deep integration. Specifically, by embedding the

signature in both the semantic and latent domains, the watermark is fundamentally woven into the image’s structure, making it far more robust to transformations than methods that only modify pixel space.

#### 3.2. Concept Decoding

As shown in Figure 2(b), the decoding stage is a two-step pipeline designed to reliably retrieve the embedded watermark and confirm its origin. First, the watermarked image ( $I_{wm}$ ) and a textual query ( $P_{query}$ ) are fed into the TokenTrace module ( $f_{tt}$ ). This textual query is a simple prompt, selected from a pre-defined set, that specifies which concept to retrieve. For example, to retrieve the <sks-object> concept, the query  $P_{query}$  would be ”a photo of <sks-object>”. The TokenTrace module then uses both inputs to predict the concept embedding ( $\tilde{e}_c$ ).

$$\tilde{e}_c = f_{tt}(I_{wm}, P_{query}) \quad (4)$$

This predicted embedding is then passed to the secret decoder ( $f_{dec}$ ), which we implement as a simple linear network. This decoder translates the high-dimensional embedding back into the original bit-secret,  $\tilde{\mathcal{S}}$ .

$$\tilde{\mathcal{S}} = f_{dec}(\tilde{e}_c) \quad (5)$$

This query-based pipeline provides a direct solution to the multi-concept challenge. By requiring a specific text query ( $P_{query}$ ) to initiate retrieval, the system can selectively isolate and verify a single concept’s signature. This mechanism allows it to successfully disentangle and attribute multiple, overlapping concepts (e.g., an object and a style) from a single image, a task that pixel-based methods cannot perform.

Importantly, the core of our retrieval mechanism is the TokenTrace module, which is architected to effectively fuse multi-modal information and predict a concept’s original embedding from a generated image. As detailed in Figure 2(c), the module is designed for parameter-efficient fine-tuning by leveraging powerful frozen pre-trained encoders from CLIP [28] for robust feature extraction. The data flow is as follows:

1. The watermarked image  $I_{wm}$  is passed through the frozen Image encoder ( $f_{img.enc}$ ). Its output features are then fed into a trainable projection layer ( $f_{proj_1}$ ) to align their dimensionality with the text features.
2. The query prompt  $P_{query}$  is passed through the frozen Text encoder ( $f_{text.enc}$ ).
3. The aligned image features and the text features are fed into a trainable attention module ( $f_{attn}$ ), which produces a fused, context-aware representation.
4. This fused representation is passed through a final trainable projection layer ( $f_{proj_2}$ ) to generate the predicted concept embedding,  $\tilde{e}_c$ .

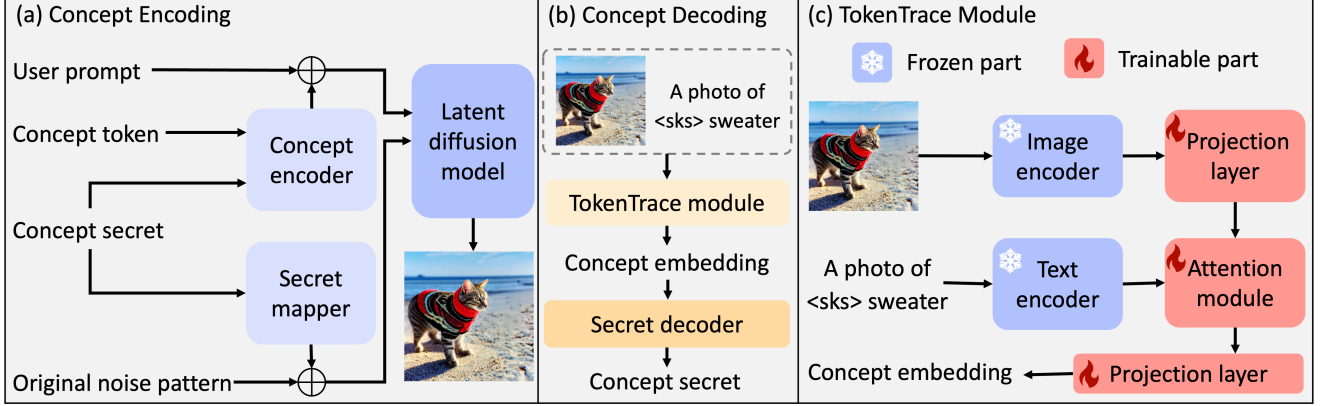


Figure 2. Overview of TokenTrace. (a) Concept encoding: A concept secret is fed into a concept encoder to perturb the targeted concept token and a secret mapper to perturb the initial noise, enabling a dual-conditioning of the latent diffusion model. (b) Concept decoding: The generated image and a query prompt are fed into the TokenTrace module to predict a concept embedding, which a secret decoder then translates back into the original concept secret for verification. (c) TokenTrace module: We use frozen image and text encoders, whose features are fused by trainable projection and attention layers to predict the final concept embedding.

This entire retrieval process is summarized by:

$$\begin{cases} F_{img} = f_{proj_1}(f_{img\_enc}(I_{wm})) \\ F_{text} = f_{text\_enc}(P_{query}) \\ F_{fused} = f_{attn}(F_{img}, F_{text}) \\ \tilde{e}_c = f_{proj_2}(F_{fused}) \end{cases} \quad (6)$$

The TokenTrace module is designed for high parameter efficiency by leveraging powerful, frozen CLIP encoders for feature extraction. This design, inspired by adapter-based finetuning [17], requires only a few lightweight projection and attention layers to be trainable. It allows the module to be adapted to new concepts quickly and scalably, avoiding the high computational cost and potential catastrophic forgetting associated with fully finetuning large-scale models.

### 3.3. Training Objective

Our training objective is to jointly optimize all trainable components: the concept encoder, secret mapper, the trainable projection and attention layers of the TokenTrace module, and the secret decoder. The model is trained using a composite loss function,  $\mathcal{L}_{total}$ , which is designed to simultaneously satisfy two competing goals: watermark retrieval accuracy and visual fidelity. This final loss is a weighted sum of four individual constraints:

- A cross-entropy loss between the original and predicted secrets to ensure the watermark can be accurately retrieved:

$$\mathcal{L}_{CE} = \text{BCE}(\mathcal{S}, \sigma(\hat{\mathcal{S}}_{logits})), \quad (7)$$

where  $\sigma$  is the sigmoid function,  $\mathcal{S}$  is the ground-truth, and  $\hat{\mathcal{S}}_{logits}$  is the output logits from the secret decoder.

- A contrastive style descriptor (CSD) loss [36] to maintain high-level semantic consistency between the water-

marked and clean images:

$$\mathcal{L}_{CSD} = 1 - \frac{\phi(I_{clean}) \cdot \phi(I_{wm})}{\|\phi(I_{clean})\| \|\phi(I_{wm})\|}, \quad (8)$$

where  $\phi$  represents the feature extractor,  $I_{clean}$  is the clean image, and  $I_{wm}$  is the watermarked image.

- A standard L2 loss to minimize perceptible, pixel-level differences between the watermarked and clean images, ensuring imperceptibility:

$$\mathcal{L}_{L2} = \|I_{clean} - I_{wm}\|_2^2. \quad (9)$$

- A regularization loss between the predicted and original concept embeddings to ensure the TokenTrace module's output is accurate:

$$\mathcal{L}_{reg} = \|e_c - \tilde{e}_c\|_2^2, \quad (10)$$

where  $e_c$  and  $\tilde{e}_c$  are the ground truth and predicted concept embeddings.

During training, the final loss is the weighted sum of these individual loss constraints, which are jointly optimized to balance watermark retrieval accuracy with visual fidelity:

$$\mathcal{L}_{total} = \lambda_1 \mathcal{L}_{CE} + \lambda_2 \mathcal{L}_{CSD} + \lambda_3 \mathcal{L}_{L2} + \lambda_4 \mathcal{L}_{reg}, \quad (11)$$

where  $\{\lambda_1, \lambda_2, \lambda_3, \lambda_4\}$  are the trade-off parameters to balance different kind of constrains. By using this composite loss function, we can jointly optimize for two competing objectives: retrieval accuracy (via  $\mathcal{L}_{CE}$  and  $\mathcal{L}_{reg}$ ) and visual fidelity (via  $\mathcal{L}_{L2}$  and  $\mathcal{L}_{CSD}$ ). This ensures the resulting watermark is both robustly detectable and imperceptible.

The end-to-end training procedure for TokenTrace is detailed in Algorithm 1 in the supplementary material. In summary, we jointly optimize all trainable parameters. In

each training iteration, we sample a batch of data (including a clean image, prompts, secret, and ground-truth embedding) and perform the concept encoding step to generate a watermarked image. This image is then passed through the decoding pipeline to retrieve the secret. Finally, we compute the total composite loss  $\mathcal{L}_{total}$  and update all trainable parameters via gradient descent. The inference (verification) process is a simple forward pass of the trained decoding modules ( $f_{tt}$  and  $f_{dec}$ ), as described in Section 3.2.

## 4. Experiments

In this section, we present a comprehensive evaluation of our proposed TokenTrace framework. We evaluate its effectiveness, scalability, and unique capability for multi-concept attribution across a diverse set of tasks: single style concept attribution, large-scale single object attribution, and compositional attribution using both customized and general concepts. We compare our framework against several state-of-the-art passive and proactive baselines and conduct a series of ablation studies to validate our key design choices.

### 4.1. Datasets

For the single style concept attribution task, we employ 23 distinct styles sourced from the WikiArt dataset [37], which is a collection of digital artworks sourced from the online art encyclopedia<sup>2</sup>. It is one of the most popular datasets for art-related computer vision tasks. For the single object concept attribution task, we use 1000 object classes from the ImageNet dataset [10], which is a foundational, large-scale dataset in computer vision. For our primary task of customized multi-concept attribution, we source pre-trained concept embeddings from the Stable Diffusion Textual Inversion Embeddings library<sup>3</sup>. This allows us to construct challenging prompts that combine multiple concepts, such as a specific object and a specific style, to test our model’s disentanglement capabilities. We also evaluate general multi-concept attribution, as composing multiple customized textual inversion embeddings in a single prompt often degrades image quality. To isolate our attribution mechanism’s performance from this generation artifact, we use standard, non-customized concepts (e.g., ”a cat and a dog”). We construct a new evaluation benchmark by using ChatGPT [6] to generate a diverse set of prompts that involve the composition of multiple concepts. For each prompt, we also generate a list of target concepts that are presented in the prompt<sup>4</sup>.

<sup>2</sup><https://www.wikiart.org/>

<sup>3</sup><https://cyberes.github.io/stable-diffusion-textual-inversion-models/>

<sup>4</sup>Specific examples can be found in supplementary material.

### 4.2. Experimental Settings

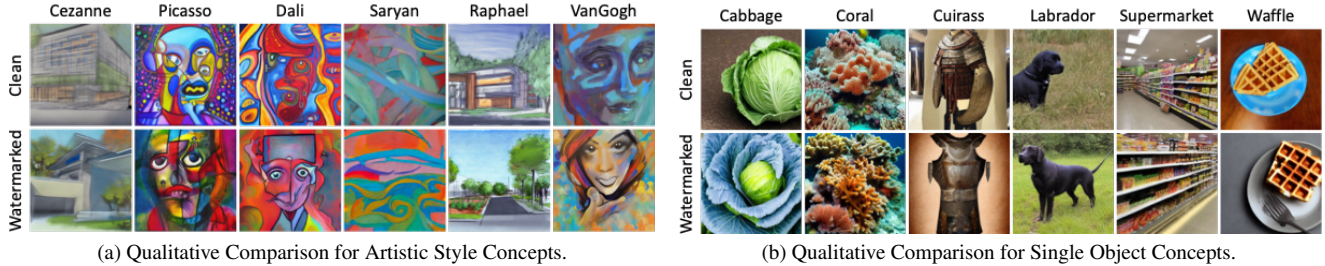
**Baselines.** We compare our method against a comprehensive suite of baselines, which are divided into two categories. The first, passive attribution, includes methods like ALADIN [32], CLIP [28], Abc [43], SSCD [27], and EK-ILA [5], which attempt to attribute a generated image after its creation by measuring visual correlation or similarity to known training data. The second, proactive attribution, includes our primary competitors, which embed a causal signature into the generative process itself. This category is represented by ProMark [2], a state-of-the-art method that embeds watermarks into the pixel domain, and Custom-Mark [3], a highly relevant baseline that, like our method, operates in the semantic domain by modifying text prompts.

**Metrics.** To evaluate our framework, we use two categories of metrics. For attribution assessment, we measure attribution accuracy, the percentage of times the predicted bit-secret exactly matches the correct ground-truth secret, and bit accuracy, the average percentage of individual bits correctly predicted. For image quality assessment, we measure the visual fidelity between the clean and watermarked images using two embedding-space metrics: the CSD Score, which is the cosine similarity between CSD descriptors to assess style preservation, and the CLIP Score, which is the cosine similarity between CLIP image embeddings to assess overall semantic similarity.

**Hyper-parameters.** We implement TokenTrace in PyTorch. For the text-to-image latent diffusion model, we use the pre-trained Stable Diffusion 1.5 [30]. For the TokenTrace module, we utilize the pre-trained ViT-L/14 encoders from CLIP [28], which remain frozen during training. Unless stated otherwise, the watermark secret  $\mathcal{S}$  is a randomly generated 16-bit binary vector. All training processes are conducted on 8 A100 NVIDIA GPUs with a batch size of 6 per GPU. All trainable parameters are optimized using the Adam optimizer with an initial learning rate of  $1e - 4$  and betas set to (0.9, 0.999). We employ a step-based learning rate schedule with a gamma of 0.95. For our composite loss function (Eq. 11), the trade-off parameters  $\{\lambda_1, \lambda_2, \lambda_3, \lambda_4\}$  were set to be  $\{5, 5, 1, 1\}$ , respectively. The model is trained for 10,000 iterations. For the final evaluation, we use the checkpoint from the last training epoch.

### 4.3. Results and Analysis

**Single Style Concept Attribution.** We first evaluate our method’s ability to attribute abstract concepts, such as artistic styles on the WikiArt [37] dataset. We compared TokenTrace against a series of both passive and proactive attribution baselines. The attribution accuracy and the bit prediction accuracy was calculated based on 100 generated images. As shown in Table 1, the results clearly demonstrate



(a) Qualitative Comparison for Artistic Style Concepts.

(b) Qualitative Comparison for Single Object Concepts.

Figure 3. Qualitative analysis of visual fidelity for watermarked images. (a) Results on abstract artistic style concepts from the WikiArt dataset. (b) Results on diverse object concepts from the ImageNet dataset. In both cases, the "Watermarked" images are visually indistinguishable from the "Clean" originals.

Table 1. Comparison of attribution performance on the WikiArt and ImageNet datasets. TokenTrace achieves the highest accuracy across both datasets, outperforming all passive and proactive baselines. "Bit" represents bit accuracy (%) and "Att." represents attribution accuracy (%). Passive baselines do not have Bit Accuracy as they do not retrieve a secret bit-string.

Method	Type	WikiArt		ImageNet	
		Bit $\uparrow$	Att $\uparrow$	Bit $\uparrow$	Att $\uparrow$
ALADIN [32]	Passive	-	18.58	-	5.55
CLIP [28]	Passive	-	52.60	-	42.61
Abc [43]	Passive	-	56.03	-	53.51
SSCD [27]	Passive	-	45.34	-	25.50
EKILA [5]	Passive	-	43.03	-	30.98
ProMark [2]	Proactive	93.14	87.19	90.56	87.30
CustomMark [3]	Proactive	95.59	89.25	93.11	87.12
<b>TokenTrace</b>	<b>Proactive</b>	<b>98.33</b>	<b>91.67</b>	<b>95.82</b>	<b>90.43</b>

Table 2. Performance comparison for multi-concept attribution. The left plot shows results for attributing 2 customized concepts (one object and one style), while the right plot shows results for 4 general concepts. TokenTrace, consistently outperforms the CustomMark baseline in both bit accuracy, represented as "Bit", and attribution accuracy, represented as "Attribution". Performance is further improved by applying prompt weighting (TokenTraceP). All accuracy metrics are in percent (%).

Method	Customized		General	
	Bit $\uparrow$	Attribution $\uparrow$	Bit $\uparrow$	Attribution $\uparrow$
CustomMark	92.47	85.14	78.93	72.78
TokenTrace	94.15	88.62	85.41	81.57
TokenTraceP	<b>96.83</b>	<b>90.53</b>	<b>90.33</b>	<b>86.08</b>

Prompt	A photo of <sks-fox>, art by <sks-Painting-style> style.		a photo of <sks-wasp> object, art by <sks-Cinematography-style> style.	
Image				
Concept	<sks-fox>	<sks-Painting-style>	<sks-wasp>	<sks-Cinematography-style>
Bit Acc.	100%	100%	100%	100%
Att. Acc.	100%	100%	100%	100%

Figure 4. Qualitative example of multi-customized concept prediction. We generate two images using a single prompt containing multiple watermarked concepts, and report the average bit accuracy and average attribution accuracy for each prompt.

the superiority of our semantic watermarking approach for this complex task.

- Firstly, TokenTrace achieves a state-of-the-art Attribution Accuracy of 91.67%, significantly outperforming all other baselines.
- Secondly, TokenTrace surpasses all passive attribution methods by a large margin. For instance, it is substantially more accurate than standard CLIP retrieval (52.60%), confirming that simple similarity is insufficient for robust attribution.
- Thirdly, our method also outperforms other proactive watermarking techniques. It shows a clear improvement over both the pixel-based ProMark (87.19%) and the latent-based CustomMark (89.25%).

The qualitative results in Figure 3a further validate our method's performance. The "Watermarked" images successfully retain the intricate details and overall aesthetic of the original artistic styles. The visual fidelity between the "Clean" and "Watermarked" pairs is high. This confirms that watermarks inserted by TokenTrace is imperceptible, a crucial requirement for any practical attribution system.

**Single Object Concept Attribution.** We further assess evaluate the scalability and performance of TokenTrace on discrete objects, we conducted a large-scale experiment on 1000 object concepts sourced from the ImageNet [10] dataset. Similar from the style attribution task, the results presented in Table 1 clearly demonstrates the superiority of our approach. TokenTrace achieves a state-of-the-art attribution accuracy of 90.43% and a bit accuracy of 95.82%. It significantly outperforms all passive methods and shows a clear performance gain over the other proactive baselines, ProMark (87.30%) and CustomMark (87.12%). The qualitative results in Figure 3b further confirm the imperceptibility of our watermark. Across diverse concepts, the "Watermarked" images are visually indistinguishable from their "Clean" images, demonstrating that TokenTrace achieves robust attribution while maintaining high visual fidelity.

**Multi-Concept Attribution.** A key advantage of our framework is attributing multiple concepts within a single image. We first evaluated this on two customized concepts on the self-created concept pool of 20 concepts (10

Prompt	a detailed cat wearing a sweater, sitting in a forest, backlit by radiant sunlight, glowing rays.			
Image				
Concept	detailed	cat	sweater	rays
Bit Acc.	90.63%	100%	100%	84.38%
Att. Acc.	75%	100%	100%	75%

Figure 5. Qualitative example of multi-general concept prediction. We generate four images using a single prompt containing multiple watermarked concepts, and report the average bit accuracy and average attribution accuracy.

objects and 10 artistic styles). As shown in Table 2, TokenTrace (88.62%) outperformed the CustomMark baseline (85.14%) upon the comparison of attribution accuracy, and an enhanced version, TokenTraceP (with prompt weighting)<sup>5</sup>, further boosted this accuracy to 90.53%. We then tested a more complex four-concept scenario. Because composing multiple customized concepts degrades image quality, we constructed a new benchmark using ChatGPT [6] to generate a diverse set of prompts involving four distinguished concepts. The results in Table 2 show our advantage becomes even more pronounced: TokenTrace (81.57%) dramatically outperformed CustomMark (72.78%) upon attribution accuracy, while TokenTraceP again achieved the highest accuracy (86.08%).

Finally, Figure 4 and Figure 5 provides qualitative proof of this disentanglement. Specifically, from a single image generated with four watermarked concepts (e.g., "detailed cat wearing a sweater... glowing rays"), our query-based module successfully retrieves the correct, independent secret for each concept, retrieving 'cat' and 'sweater' with 100% accuracy and 'detailed' and 'rays' with high accuracy. This confirms our query-based mechanism solves concept overlap and scales to complex, compositional prompts. More qualitative examples can be found in the supplementary material.

**Sequential Learning.** To evaluate our framework’s ability to add new concepts without full retraining, we perform a sequential learning experiment on the WikiArt dataset. We first train an initial TokenTrace model on 10 style concepts, then sequentially introduce 2 new concepts at a time up to 20. Critically, we do not retrain from scratch but instead finetune the existing model with only 10% additional iterations per step, reflecting a real-world scenario. The results in Figure 6 demonstrate high efficiency and strong resistance to catastrophic forgetting. Both Attribution Accuracy (starting at 98.22% and ending at 94.13%) and CSD Score (starting at 0.91 and ending at 0.84) remain high, confirming that our parameter-efficient design can be dynamically updated, making it a scalable and practical solution.

<sup>5</sup>Details about TokenTraceP can be found in supplementary material.

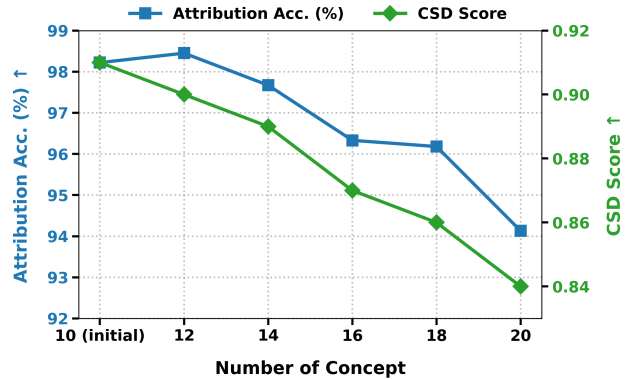


Figure 6. Performance on incremental concept learning. The plot shows the attribution accuracy (left y-axis, blue squares) and CSD score (right y-axis, green diamonds) as new concepts are sequentially added to a pre-trained model. The results demonstrate that both attribution accuracy and visual fidelity remain high, showing the method’s efficiency in real-world applications.

#### 4.4. Ablation Studies

**Ablation on Loss Components.** Our composite loss function ( $\mathcal{L}_{total}$ ), as defined in Eq. 11, is designed to jointly optimize for retrieval accuracy and visual fidelity. To demonstrate the contribution of each loss term, we train our model from scratch with different components of the objective function removed. The full model ("All") is trained with all loss components, including  $\mathcal{L}_{CE}$ ,  $\mathcal{L}_{CSD}$ ,  $\mathcal{L}_{L2}$ , and  $\mathcal{L}_{reg}$ . As shown in Table 3, our complete model ("All") achieves the best performance. Removing the CSD loss ("No CSD") causes the most significant performance drop. This finding confirms that the  $\mathcal{L}_{CSD}$  term is critical for maintaining the high-level semantic and style consistency required for accurate retrieval. Removing the image-space L2 loss ("No L2 (Image)") also leads to a notable decrease in performance, with attribution accuracy dropping to 86.37% and the CSD Score falling to 0.73. The latent-space L2 ("No L2 (Latent)") also contributes, with its removal dropping accuracy to 88.52%.

**Ablation on Bit Secret Length.** We next investigate the impact of the length of the bit secret  $\mathcal{S}$ , on both attribution accuracy and visual fidelity. We trained separate models on the WikiArt dataset using secret lengths of 5, 8, 16 (our default), 32, and 64 bits. As shown in Figure 7, we observe a clear and expected trade-off between information capacity and performance. Specifically, The model achieves the highest attribution accuracy (94.38%) with a 5-bit secret, as this smaller signal is easiest to embed and retrieve. As the bit length increases, all metrics show a graceful degradation. When moving from our 16-bit default to a 64-bit secret, the attribution accuracy drops from 91.67% to 84.18%, and the CSD score falls from 0.82 to 0.72. This trend is logical, as embedding a larger and more complex signal (64 bits) into the image is an inherently harder optimization problem

Table 3. Ablation study for the objective function on the WikiArt dataset. Our full model (“All”) significantly outperforms variants where individual loss components (CSD, Latent L2, Image L2) are removed, demonstrating that each component is necessary for achieving both high attribution accuracy and visual fidelity.

Attribution Performance (%)		
Method	Bit Acc. $\uparrow$	Attribution Acc. $\uparrow$
No CSD	91.81	83.75
No L2 (latent)	96.03	88.52
No L2 (Image)	93.65	86.37
<b>All</b>	<b>98.33</b>	<b>91.67</b>

Image Quality		
Method	CLIP Score $\uparrow$	CSD Score $\uparrow$
No CSD	0.73	0.65
No L2 (latent)	0.82	0.76
No L2 (Image)	0.81	0.73
<b>All</b>	<b>0.87</b>	<b>0.82</b>

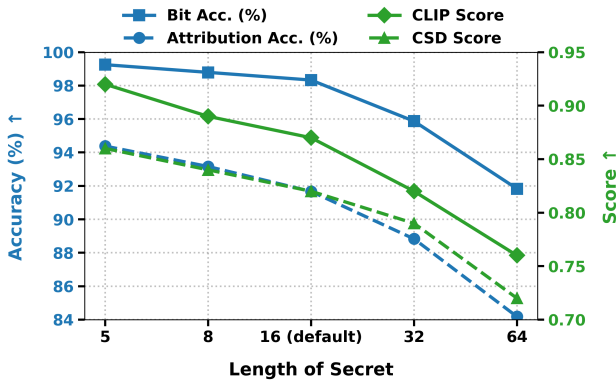


Figure 7. Ablation study for the length of the bit secret on the WikiArt dataset. Performance shows a graceful trade-off between capacity and accuracy. Our 16-bit default provides the best balance of high attribution accuracy and visual fidelity.

and is more likely to interfere with the image’s original semantic content, thus slightly reducing visual fidelity. These findings validate our choice of 16 bits as the default, as it provides an balance, offering a sufficiently large space for unique signatures while maintaining both high attribution accuracy and high visual quality.

**Ablation on the Number of Concepts.** We next evaluate our framework’s scalability by training models on the ImageNet dataset with concept pools of increasing size: 10, 100, 500, and 1000 concepts. The results in Figure 8 demonstrate a very high level of performance and graceful degradation. As the concept library scales from 10 to 1000 concepts, the attribution accuracy remains exceptionally high, dropping only 6 percentage points (96.39%  $\rightarrow$  90.43%). Similarly, bit accuracy shows strong resilience (99.16%  $\rightarrow$  95.82%), and visual fidelity scales well, with the CSD score dropping only from 0.84 to 0.71. These findings demonstrate that TokenTrace is highly scalable and can robustly handle a large library of distinct concepts, confirm-

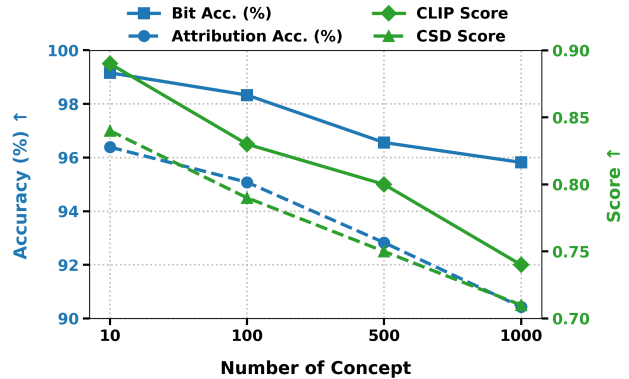


Figure 8. Ablation study for the number of concepts on the ImageNet dataset. Performance remains high and degrades gracefully as the number of concepts scales from 10 to 1000, demonstrating the high scalability of our method.

ing its practicality for real-world applications.

**Robustness to Image Distortions.** Finally, to validate our watermark’s resilience, we conducted a robustness analysis by applying common image distortions to watermarked WikiArt images before retrieval, simulating real-world re-encoding and editing. The results in Table 4 demonstrate that our dual-conditioning strategy creates a highly robust watermark. The method shows exceptional resilience, maintaining over 90.04% attribution accuracy against Rotation and over 87% against both JPEG compression and a targeted Adversarial Attack. Performance also degrades gracefully for more severe transformations, with CropAndResize (86.57%), GaussianBlur (84.81%), ColorJitter (83.22%), and GaussianNoise (82.94%) all retaining over 82% accuracy. These results confirm that by embedding the signature in both the semantic and latent domains, our watermark is a deeply integrated signal, allowing for reliable attribution even after significant image alterations.

Table 4. Ablation study for different types of distortions on the WikiArt dataset. Our method demonstrates high robustness, maintaining strong attribution accuracy even after significant image transformations.

Method	Bit Acc. $\uparrow$	Attribution Acc. $\uparrow$
No distortion	98.33	91.67
JPEG	94.68	88.20
Rotation	96.21	90.04
CropAndResize	93.28	86.57
GaussianBlur	91.32	84.81
GaussianNoise	89.18	82.94
ColorJitter	89.62	83.22
Sharpness	92.71	86.54
Adversarial Attack [51]	94.08	87.17

## 5. Conclusion

In this paper, we introduced TokenTrace, a novel proactive watermarking framework that solves the challenging task of multi-concept attribution. By embedding a secret into both the textual semantic and latent domains, our method creates a robust signature that avoids the spatial overlap problem plaguing pixel-based methods. Our key contribution is the query-based TokenTrace module, which can successfully disentangle and independently retrieve signatures for multiple, composed concepts from a single image. Extensive experiments demonstrate that TokenTrace significantly outperforms state-of-the-art baselines on single-concept (style and object) and multi-concept tasks, all while maintaining high visual fidelity and robustness to distortions.

# TokenTrace: Multi-Concept Attribution through Watermarked Token Recovery

## Supplementary Material

### 6. Detailed Algorithm for TokenTrace

The end-to-end training procedure for TokenTrace is summarized in Algorithm 1. We jointly optimize all trainable parameters, denoted by  $\{\theta_{enc}, \theta_{map}, \theta_{pb}, \theta_{dec}\}$ . In each training iteration, we sample a batch of data containing a clean image ( $I_{clean}$ ), its corresponding prompts ( $P_{user}$ ) that contains the concept prompt ( $P_{concept}$ ), a secret ( $\mathcal{S}$ ), and the ground-truth concept embedding ( $E_{concept}$ ). We first perform the concept encoding step to generate the perturbed inputs and produce a watermarked image. Then, we pass this image through the decoding pipeline to retrieve the secret. Finally, we compute the total composite loss  $\mathcal{L}_{total}$  and update all trainable parameters via gradient descent.

---

#### Algorithm 1 TokenTrace Training

---

**Require:** Trainable parameters  $\theta_{enc}, \theta_{map}, \theta_{pb}, \theta_{dec}$ ; Loss weights  $\lambda_1, \lambda_2, \lambda_3, \lambda_4$

- 1: **for** each training step **do**
- 2:     **1. Concept Encoding & Generation**
- 3:     Sample batch ( $I_{clean}, P_{user}, P_{concept}, \mathcal{S}, E_{concept}$ )
- 4:      $E_{prompt} \leftarrow \text{Embed}(P_{user})$
- 5:      $\hat{E}_{prompt} \leftarrow E_{prompt} + f_{enc}(E_{concept}, \mathcal{S})$
- 6:     Sample initial noise  $z_T \sim \mathcal{N}(0, 1)$
- 7:      $\hat{z}_T \leftarrow z_T + f_{map}(\mathcal{S})$
- 8:      $I_{wm} \leftarrow DM(\hat{z}_T, \hat{E}_{prompt})$
- 9:     **2. Concept Decoding & Verification**
- 10:      $P_{query} \leftarrow P_{concept}$      ▷ or  $P_{user}$  as query
- 11:      $\tilde{E}_{concept} \leftarrow f_{pb}(I_{wm}, P_{query})$
- 12:      $\tilde{s}_{logits} \leftarrow f_{dec}(\tilde{E}_{concept})$
- 13:     **3. Loss Calculation**
- 14:      $\mathcal{L}_{CE} \leftarrow \text{BCE}(\mathcal{S}, \sigma(\tilde{s}_{logits}))$
- 15:      $\mathcal{L}_{L2} \leftarrow \|I_{clean} - I_{wm}\|_2^2$
- 16:      $\mathcal{L}_{CSD} \leftarrow 1 - \text{sim}(\phi(I_{clean}), \phi(I_{wm}))$
- 17:      $\mathcal{L}_{reg} \leftarrow \|E_{concept} - \tilde{E}_{concept}\|_2^2$
- 18:      $\mathcal{L}_{total} \leftarrow \lambda_1 \mathcal{L}_{CE} + \lambda_2 \mathcal{L}_{CSD} + \lambda_3 \mathcal{L}_{L2} + \lambda_4 \mathcal{L}_{reg}$
- 19:     **4. Optimization**
- 20:     Update  $\theta_{enc}, \theta_{map}, \theta_{pb}, \theta_{dec}$  using  $\nabla_{\theta} \mathcal{L}_{total}$
- 21: **end for**

---

For the inference there are two processes: watermark generation, as shown in Algorithm 2, and concept attribution, as shown in Algorithm 3. The watermarking process begins during image generation using a dual-conditioning strategy. A unique binary secret  $\mathcal{S}$  is assigned to the target concept. This secret is processed by two parallel networks: a concept encoder, which generates a perturbation embedding that is fused with the user’s text prompt embedding, and a secret mapper, which generates a structured

noise pattern that is fused with the initial gaussian noise. The latent diffusion model is then conditioned on these two perturbed inputs, modifying both the textual semantic and latent domains, to synthesize the final watermarked image  $I_{wm}$ , deeply integrating the signature into the content. Concept attribution is performed as a targeted retrieval operation. Given a suspect image  $I_{wm}$  and a specific concept to verify, we construct a corresponding textual query  $P_{query}$  (e.g., "a photo of <sks-object>"). These inputs are fed into the trained TokenTrace module, where frozen CLIP encoders extract multi-modal features that are aligned and fused by learned projection and attention layers to predict the target concept embedding,  $\tilde{E}_{concept}$ . This predicted embedding is passed through the secret decoder to recover the binary secret  $\tilde{s}$ . Attribution is confirmed by comparing this retrieved sequence against the ground-truth secret; a high bit-match rate provides cryptographic-like proof that the specific concept was used during generation.

---

#### Algorithm 2 TokenTrace Watermarking (Generation)

---

**Require:** Trained parameters  $\theta_{enc}, \theta_{map}$

**Require:** User prompt  $P_{user}$ , Concept prompt  $P_{concept}$ , Secret  $\mathcal{S}$

**Ensure:** Watermarked Image  $I_{wm}$

- 1: **1. Semantic Perturbation**
- 2:  $E_{prompt} \leftarrow \text{Embed}(P_{user})$      ▷ Get initial prompt embeddings
- 3:  $\Delta E \leftarrow f_{enc}(E_{concept}, \mathcal{S})$      ▷ Generate concept perturbation
- 4:  $\hat{E}_{prompt} \leftarrow E_{prompt} + \Delta E$      ▷ Fuse perturbation with target token
- 5: **2. Latent Perturbation**
- 6: Sample initial noise  $z_T \sim \mathcal{N}(0, 1)$
- 7:  $\Delta z \leftarrow f_{map}(\mathcal{S})$      ▷ Generate noise perturbation
- 8:  $\hat{z}_T \leftarrow z_T + \Delta z$      ▷ Fuse perturbation with initial noise
- 9: **3. Generation**
- 10:  $I_{wm} \leftarrow DM(\hat{z}_T, \hat{E}_{prompt})$      ▷ Generate image using diffusion model
- 11: **return**  $I_{wm}$

---

### 7. Details of TokenTraceP

This section provides the technical details for our enhanced model variant, TokenTraceP, which is featured in our multi-concept attribution experiments.

In our multi-concept experiments, we evaluate the model’s ability to attribute multiple concepts (e.g., an object and a style) composed in a single prompt. A well-known

---

**Algorithm 3** TokenTrace Inference (Attribution)

---

**Require:** Trained parameters  $\theta_{tt}, \theta_{dec}$ **Require:** Input image  $I_{wm}$ , Query prompt  $P_{query}$ , Ground-truth secret  $\mathcal{S}_{GT}$ **Ensure:** Retrieved Secret  $\tilde{s}$ , Attribution Decision

- 1: **1. Concept Decoding**
  - 2:  $\tilde{E}_{concept} \leftarrow f_{tt}(I_{wm}, P_{query})$   $\triangleright$  Predict concept embedding using query
  - 3:  $\tilde{s}_{logits} \leftarrow f_{dec}(\tilde{E}_{concept})$   $\triangleright$  Predict raw logits
  - 4: **2. Secret Recovery**
  - 5:  $\tilde{s}_{prob} \leftarrow \sigma(\tilde{s}_{logits})$   $\triangleright$  Apply Sigmoid function
  - 6:  $\tilde{s} \leftarrow (\tilde{s}_{prob} > 0.5)$   $\triangleright$  Binarize to obtain retrieved bit-secret
  - 7: **3. Verification**
  - 8:  $Score \leftarrow \text{BitAccuracy}(\tilde{s}, \mathcal{S}_{GT})$   $\triangleright$  Compare with ground truth
- 

challenge in generative customization is "concept overpowering" [7, 31], where one concept in a prompt (typically the object) visually dominates the generation, while the other (typically the style) is rendered less faithfully. This weak rendering of the style concept is not just a visual quality issue; it directly impacts attribution. A poorly-rendered style provides a weaker signal for our TokenTrace module to detect, leading to lower retrieval accuracy for that concept's secret.

To address this, our enhanced TokenTraceP variant integrates prompt weighting<sup>6</sup>, a common technique in the diffusers library to "increase or decrease the scale of the text embedding vector" for a specific concept. This method is applied only during the generation of the watermarked image ( $I_{wm}$ ). In our standard TokenTrace encoding, the final watermarked text embedding  $\hat{E}_{prompt}$  is a collection of tokens, including the perturbed object token  $\hat{e}_{object}$  and the perturbed style token  $\hat{e}_{style}$ :

$$\begin{cases} \hat{e}_{object} = e_{object} + f_{enc}(e_{object}, \mathcal{S}_{object}) \\ \hat{e}_{style} = e_{style} + f_{enc}(e_{style}, \mathcal{S}_{style}) \\ \hat{E}_{prompt} = \{e_1, \dots, \hat{e}_{object}, \dots, \hat{e}_{style}, \dots, e_k\} \end{cases} \quad (12)$$

For the TokenTraceP variant, we apply an additional scaling factor  $\alpha > 1.0$  (we set  $\alpha$  equals to 1.1 by default in the experiments conducted in main paper) specifically to the style token's embedding after our perturbation. This new, weighted style token  $\hat{e}_{style\_P}$  is calculated as:

$$\hat{e}_{style\_P} = \alpha \times \hat{e}_{style} \quad (13)$$

The final prompt embedding  $\hat{E}_{prompt\_P}$  sent to the diffusion

---

<sup>6</sup>[https://huggingface.co/docs/diffusers/v0.21.0/en/using-diffusers/weighted\\_prompts](https://huggingface.co/docs/diffusers/v0.21.0/en/using-diffusers/weighted_prompts)

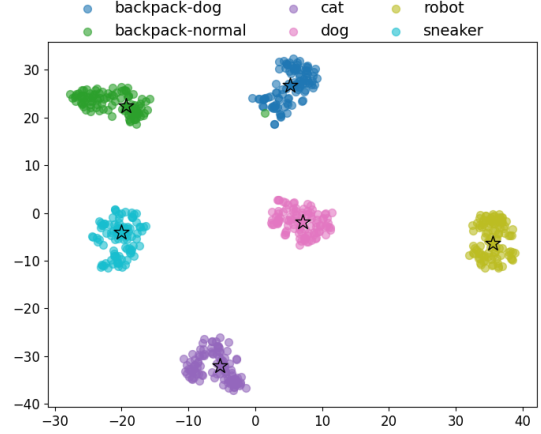


Figure 9. t-SNE visualization of predicted concept embeddings. The plot shows that embeddings retrieved by our TokenTrace module from DreamBooth-generated images (dots) form distinct, well-separated clusters around the corresponding ground-truth embeddings (stars), validating its ability to perform concept attribution.

model then uses this amplified style token:

$$\hat{E}_{prompt\_P} = \{e_1, \dots, \hat{e}_{object}, \dots, \hat{e}_{style\_P}, \dots, e_k\} \quad (14)$$

This re-weighting forces the diffusion model's cross-attention layers to focus more on the style concept, ensuring it is rendered more robustly and faithfully alongside the dominant object.

## 8. Preliminary explorations of TraceToken module

Before training our full end-to-end framework, we conducted a preliminary experiment to validate the core hypothesis of our method: whether the TokenTrace module can learn to extract distinct, coherent concept embeddings from generated images. To isolate the module's retrieval capability, we first trained the TokenTrace module using real images from the DreamBooth dataset<sup>7</sup>. This dataset contains sets of images for various unique concepts (e.g., "cat," "dog," "sneaker"). After this initial training, we used the official DreamBooth [31] model itself to generate 100 novel images for each of these concepts. We then fed these generated images into our trained TokenTrace module to predict their corresponding concept embeddings. Finally, to visualize the high-dimensional embedding space, we applied t-SNE [24] to reduce the dimension of the predicted embeddings.

The t-SNE visualization of the predicted embeddings is shown in Figure 9. The results clearly demonstrate that the TokenTrace module is highly effective at this retrieval task. As can be observed:

---

<sup>7</sup><https://github.com/google/dreambooth>

- Embeddings predicted from images of the same concept (dots) form tight, well-defined clusters around their corresponding ground-truth embeddings (stars, derived from real images).
- Embeddings from different concepts (e.g., 'sneaker' vs. 'robot') are well-separated in the feature space, forming distinct and non-overlapping distributions.

This successful separation confirms that our TokenTrace module can effectively learn to map generated images back to their underlying conceptual representations. This preliminary result validated our hypothesis that using a predicted concept embedding as the basis for secret retrieval is a feasible and promising approach for concept attribution.

## 9. General Multi-Concept Attribution Dataset

In our main experiments, we evaluate multi-concept attribution on customized concepts (e.g., specific objects and styles) learned via textual inversion. A well-known limitation of this approach is that image quality and concept coherence degrade significantly when more than two customized embeddings are composed in a single prompt. To test the scalability of our attribution mechanism on more complex prompts (e.g., four distinct concepts) without this confounding generation-quality artifact, we created a new benchmark using general, non-customized concepts. This dataset allows us to evaluate the core hypothesis: can TokenTrace disentangle and retrieve multiple, independent secrets from a single, coherently-generated image?

We constructed this benchmark using ChatGPT. We prompted the model to generate a diverse set of descriptive sentences, each containing four distinct and clear concepts (objects, attributes, etc.). For each generated prompt, we also instructed the model to extract a corresponding list of four key "target" concepts. Each entry in the dataset consists of a prompt string and a targets list. The prompt is used for the image generation step, and the targets list provides the individual concepts to be queried and retrieved by our TokenTrace module. Below are several representative examples from the dataset: Below are several representative examples from the dataset:

```

1 [
2   {
3     "prompt": "a cat wearing a sweater
4     sitting on a sunny beach",
5     "targets": ["cat", "sweater", "
6     sunny", "beach"]
7   },
8   {
9     "prompt": "a bird flying above
10    snowy mountains under a blue sky",
11    "targets": ["bird", "snowy", "
12    mountains", "sky"]
13  },

```

```

14  {
15    "prompt": "a musician playing piano
16    in a hall with a dog beside",
17    "targets": ["musician", "piano", "
18    hall", "dog"]
19  },
20  {
21    "prompt": "a fox sitting beside a
22    glowing campfire at night",
23    "targets": ["fox", "glowing", "
24    campfire", "night"]
25  },
26  {
27    "prompt": "a woman tightly holding
28    an umbrella while walking through the
29    heavy rain",
30    "targets": ["women", "umbrella", "
31    heavy", "rain"]
32  },
33  ...
34 ]

```

Listing 1. Example entries from our self-constructed general multi-concept dataset. Each entry contains a generation prompt and a list of target concepts for retrieval.

In our experiment, each general concept in the target vocabulary (e.g., "cat," "dog," "sweater," "beach") is pre-associated with its own unique, learnable secret. This dataset allows us to generate a single image using the full prompt and then iteratively query the TokenTrace module with each of the four target words to verify that all four distinct secrets can be successfully and independently retrieved.

## 10. Comprehensive Attribution and Security Test

To provide a final, rigorous evaluation of our method's overall performance and security, we conduct a comprehensive attribution test that jointly evaluates the True Positive Rate (TPR) and the False Positive Rate (FPR). We construct a large test set ( $X_{test}$ ) composed equally of watermarked images ( $I_{wm}$ ) and zero-watermark clean images ( $I_{clean}$ ), and query every image for the same known secret ( $S_{GT}$ ). This test measures the following key metrics:

- Effectiveness (TPR): The percentage of times the system correctly attributes the secret to a watermarked image ( $I_{wm}$ ).
- Security (FPR): The percentage of times the system incorrectly attributes the secret to a clean image ( $I_{clean}$ ). For a robust system, this value must be near zero.
- Overall Performance ( $F_1$  Score): A balanced harmonic mean of precision and recall, demonstrating the system's overall viability.

The results confirm that TokenTrace achieves excellent

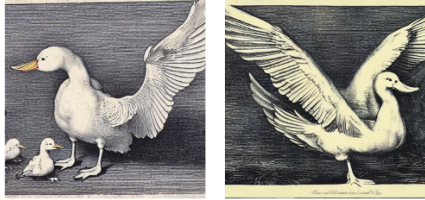
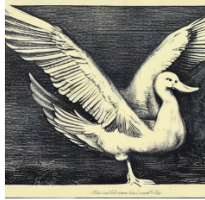
<b>Prompt</b>	a photo of <sks-Aflac-duck> object, art by <sks-durer-style> style.		a photo of <sks-Aflac-duck> object, art by <sks-hanfu-anime-style> style.	
<b>Image</b>				
<b>Concept</b>	<sks-Aflac-duck>	<sks-durer-style>	<sks-Aflac-duck>	<sks-hanfu-anime-style>
<b>Bit Acc.</b>	100%	100%	100%	100%
<b>Att. Acc.</b>	100%	100%	100%	100%

Figure 10. Qualitative example of multi-customized concept prediction. We generate two images for each prompt containing multiple watermarked concepts, and report the average bit accuracy and average attribution accuracy.

<b>Prompt</b>	a photo of <sks-cheburashka> object, art by <sks-hanfu-anime-style> style.		a photo of <sks-babau> object, art by <sks-hanfu-anime-style> style.	
<b>Image</b>				
<b>Concept</b>	<sks-cheburashka>	<sks-hanfu-anime-style>	<sks-babau>	<sks-hanfu-anime-style>
<b>Bit Acc.</b>	100%	100%	100%	100%
<b>Att. Acc.</b>	100%	100%	100%	100%

Figure 11. Qualitative example of multi-customized concept prediction. We generate two images for each prompt containing multiple watermarked concepts, and report the average bit accuracy and average attribution accuracy.

performance and perfect security on this comprehensive test. We measured the True Positive Rate (TPR) at 92.75% and the False Positive Rate (FPR) at 0.00%. The resulting F<sub>1</sub> Score is 96.20%. This zero-FPR indicates that the model is highly specific, learning the unique, embedded signature and not general noise, confirming the integrity and high security of our causal attribution mechanism.

## 11. Qualitative Examples on Multi-Concept Attribution

In this section, we provide additional qualitative examples to further demonstrate the effectiveness and robustness of our TokenTrace framework. These examples supplement the multi-concept attribution results presented in the main paper, showing our method’s ability to disentangle and independently retrieve secrets for both customized and general concepts.

Figure 10 and Figure 11 show two additional examples of compositional attribution for customized concepts

sourced from the Textual Inversion library. In each case, an image is generated from a prompt that combines a specific object concept and a specific style concept. As the results demonstrate, when the single composite image is queried with a prompt for the object, it correctly retrieves the object’s secret. When the same image is queried with a prompt for the style, it correctly retrieves the style’s secret. This confirms our method’s ability to disentangle customized, overlapping concepts.

Figure 12 and Figure 13 show two additional examples of attribution for general concepts. These images were generated from complex prompts containing multiple watermarked keywords (e.g., "cat," "sweater," "beach"). The results provide further evidence that our query-based TokenTrace module can successfully isolate and retrieve the correct, distinct secret for each general concept, even when they are composed in a single image.

Figure 14 and Figure 15 provide additional qualitative analysis, demonstrating both the strong disentanglement ca-

<b>Prompt</b>	a woman tightly holding an umbrella while walking through the heavy rain.			
<b>Image</b>				
<b>Concept</b>	women	umbrella	heavy	rain
<b>Bit Acc.</b>	100%	100%	78.13%	90.63%
<b>Att. Acc.</b>	100%	100%	50%	75%

Figure 12. Qualitative example of multi-customized concept prediction. We generate four images for each prompt containing multiple watermarked concepts, and report the average bit accuracy and average attribution accuracy.

<b>Prompt</b>	a musician playing piano in a hall with a dog beside.			
<b>Image</b>				
<b>Concept</b>	musician	piano	hall	dog
<b>Bit Acc.</b>	100%	100%	100%	100%
<b>Att. Acc.</b>	100%	100%	100%	100%

Figure 13. Qualitative example of multi-customized concept prediction. We generate four images for each prompt containing multiple watermarked concepts, and report the average bit accuracy and average attribution accuracy.

pability of the TokenTrace module and the performance boundaries related to concept abstractness. The experiments show that retrieval success is contingent on the faithfulness of the concept’s visual representation by the underlying generative model.

In both complex prompts, all primary, high-priority concepts, such as the stylistic attribution ‘Dali’ (100% Att. Acc.) or the object ‘dog’ and accessory ‘sunglasses’ (both 100% Att. Acc.), are retrieved perfectly, confirming the module’s core disentanglement strength. However, both figures illustrate a clear performance drop for non-dominant, abstract, or atmospheric concepts:

- In the road scene (Figure 14), the abstract attribute ‘sunny’ has the lowest retrieval rate (60% Att. Acc.).
- In the landscape scene (Figure 15), the general environmental concept ‘hills’ also achieves the lowest retrieval rate (60% Att. Acc.).

This pattern confirms that when the diffusion model struggles to robustly ground an abstract concept in the visual output, the corresponding visual features are weak, which in turn diminishes the semantic signal for the TokenTrace

module’s frozen CLIP encoders to capture. This highlights a boundary condition of our method: while highly effective, successful retrieval remains contingent on the visual clarity of the concept rendered by the generative model.

## 12. Qualitative Analysis on Complex Prompts

This section presents a qualitative analysis of TokenTrace’s performance on images generated from complex, descriptive prompts, utilizing the WikiArt dataset. We compare the visual fidelity of “clean” images (left in each pair) against their “watermarked” counterparts (right in each pair). Our primary goal with this analysis is to visually confirm that our dual-conditioning embedding strategy introduces minimal perceptible degradation to the generated images, even when the prompts are intricate and aim for specific artistic styles or detailed scenes. Each example highlights a prompt designed to elicit a rich visual output, varying in subject matter, artistic style, and atmospheric conditions.

As evident from the Figure 16, the watermarked images consistently maintain high visual quality, faithfully representing the aesthetic and thematic intentions of the origi-

<b>Prompt</b>	A peaceful and breathtaking landscape painting in the signature style of <b>Dali</b> , illustrating rolling green <b>hills</b> , a tranquil <b>lake</b> reflecting the sky, distant <b>mountains</b> softened by mist, and multiple <b>trees</b> .				
<b>Image</b>					
<b>Concept</b>	Dali	hills	lake	mountains	trees
<b>Bit Acc.</b>	100%	76.25%	87.5%	100%	100%
<b>Att. Acc.</b>	100%	60%	80%	100%	100%

Figure 14. Disentanglement of Concrete Concepts and Attributes. Per-concept retrieval accuracy for the complex road scene prompt. Prominent concepts (dog, sunglasses) are recovered at 100% accuracy, while the abstract attribute 'sunny' shows the lowest retrieval rate (60%), confirming performance dependency on visual clarity.

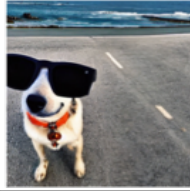
<b>Prompt</b>	on a <b>sunny</b> road beside the <b>ocean</b> , a <b>dog</b> wearing <b>sunglasses</b> stands confidently as the sea breeze blows past.				
<b>Image</b>					
<b>Concept</b>	sunny	road	ocean	dog	sunglass
<b>Bit Acc.</b>	77.5%	100%	90%	100%	100%
<b>Att. Acc.</b>	60%	100%	80%	100%	100%

Figure 15. Disentanglement of Abstract Styles and Environmental Concepts. Per-concept retrieval accuracy for the complex landscape prompt. Primary concepts ('Dali' style, mountains) are recovered perfectly, while the general environmental concept 'hills' shows the lowest retrieval rate (60%), illustrating the performance boundary for general, non-dominant concepts.

nal prompts. Details such as rolling hills, towering waves, mystical landscapes, and historical figures are preserved with remarkable consistency. The subtle perturbations introduced by TokenTrace, which are embedded in both the textual semantic and latent domains, do not lead to noticeable artifacts, blurring, or distortion, thus validating that our method achieves robust watermarking without compromising the generative model's artistic capabilities. This visual assessment reinforces the quantitative metrics presented in the main paper regarding image quality (e.g., CSD scores).

### 13. Image Fidelity Analysis (FID)

To evaluate the impact of watermarking on the overall generation quality, we measure the Fréchet Inception Distance (FID) [16] on the ImageNet dataset. A lower FID score indicates that the generated images are closer to the distribution of real images.

The results for the baseline methods are presented in Table 5. As expected, any proactive watermarking method

necessarily introduces some degradation compared to the Original LDM (FID 13.28).

- ProMark (a pixel-based method) results in a severe drop in image quality, yielding the highest FID score of 17.63.
- The FID score for TokenTrace is 14.98. This result confirms that semantic methods (TokenTrace/CustomMark) are vastly superior to pixel-based watermarking (ProMark), as TokenTrace introduces minimal degradation relative to the Original LDM baseline. TokenTrace maintains image quality that is highly comparable to CustomMark.

This finding confirms that the semantic approach used by both CustomMark and TokenTrace is significantly less detrimental to overall image fidelity than global pixel-level watermarking.

### 14. Prompt Details

This section details the standardized prompt templates used in our single-concept and multi-concept experiments, fol-

A peaceful and breathtaking landscape painting in the signature style of **Dali**, illustrating rolling green hills, a tranquil lake reflecting the sky, and distant mountains softened by mist.



A dramatic and intense seascape painting by **Rembrandt**, where towering waves clash against jagged rocks under a sky filled with lightning, evoking nature's raw power.



A mesmerizing and deeply immersive painting by **Monet**, using cool tones and surreal elements to depict a dreamlike world filled with floating islands and cascading waterfalls.



A serene and nostalgic winter landscape, painted by **Raphael**, featuring a frozen river, bare trees covered in frost, and warm golden light peeking through a cloudy sky.



A breathtaking and imaginative painting of a mystical island, painted by **VanGogh**, where waterfalls cascade from floating cliffs, glowing flora illuminates the night.



A deeply evocative portrait of a renowned historical figure, painted in the signature style of **Cezanne**, where the subject's gaze and finely detailed clothing reflect their era.



Figure 16. Qualitative comparison of images generated from complex prompts on the WikiArt dataset. For each pair, the left image is the clean (unwatermarked) version, and the right image is the watermarked version generated by TokenTrace. Our method consistently maintains high visual fidelity and adherence to the prompt, even for intricate artistic scenes.

Table 5. Comparison of Fréchet Inception Distance (FID) scores on the ImageNet dataset. Lower FID indicates higher image fidelity.

Method	FID ↓
Original LDM	13.28
ProMark	17.63
CustomMark	14.73
<b>TokenTrace</b>	<b>14.98</b>

lowing the approach for training customized embeddings (e.g., CustomMark [3]).

Following is the complete list of standardized prompt templates used in our single-concept attribution experiments:

1. Prompts used during training for single style concept attribution. The [name] placeholder is replaced by the specific watermarked tokens during the experiment.

- a painting, art by [name]
- a rendering, art by [name]
- a cropped painting, art by [name]
- the painting, art by [name]
- a clean painting, art by [name]
- a dirty painting, art by [name]
- a dark painting, art by [name]
- a picture, art by [name]
- a cool painting, art by [name]
- a close-up painting, art by [name]

- a bright painting, art by [name]
- a rendition, art by [name]
- a nice painting, art by [name]
- a small painting, art by [name]
- a weird painting, art by [name]
- a large painting, art by [name]
- a serene landscape painting in the style of [name]
- a bustling cityscape in the style of [name]
- a painting of a cozy cottage in the woods in the style of [name]
- a vibrant underwater scene in the style of [name]
- a whimsical painting of a flying elephant in the style of [name]
- a still life painting featuring fruit and flowers in the style of [name]
- a portrait of a famous historical figure in the style of [name]
- a painting of a dreamy night sky in the style of [name]
- a colorful abstract painting in the style of [name]
- a street scene from Paris in the style of [name]
- a depiction of a beautiful sunset over the ocean in the style of [name]
- a painting of a peaceful mountain village in the style of [name]
- an energetic painting of dancers in motion in the style of [name]
- a painting of a snow-covered winter scene in the style of [name]

- a painting of a tropical paradise in the style of [name]
- a painting of a magical forest filled with fantastical creatures in the style of [name]
- a painting of a dramatic stormy seascape in the style of [name]
- a portrait of a majestic lion in the style of [name]
- a painting of a romantic scene between two lovers in the style of [name]
- a painting of a serene Japanese garden in the style of [name]
- a painting of a bustling marketplace in the style of [name]
- a painting of a tranquil river scene in the style of [name]
- a painting of a fiery volcano eruption in the style of [name]
- a painting of a futuristic cityscape in the style of [name]
- a painting of a whimsical circus scene in the style of [name]
- a painting of a mysterious moonlit forest in the style of [name]
- a painting of a dramatic desert landscape in the style of [name]
- a portrait of a regal peacock in the style of [name]
- a painting of a mystical island in the style of [name]
- a painting of a lively carnival scene in the style of [name]

2. Prompts used during training for single object concept attribution. The [name] placeholder is replaced by the specific watermarked tokens during the experiment.

- a photo of a [name]
- a rendering of a [name]
- a cropped photo of the [name]
- the photo of a [name]
- a photo of a clean [name]
- a photo of a dirty [name]
- a dark photo of the [name]
- a photo of my [name]
- a photo of the cool [name]
- a close-up photo of a [name]
- a bright photo of the [name]
- a cropped photo of a [name]
- a photo of the [name]
- a good photo of the [name]
- a photo of one [name]
- a close-up photo of the [name]
- a rendition of the [name]
- a photo of the clean [name]
- a rendition of a [name]
- a photo of a nice [name]
- a good photo of a [name]
- a photo of the nice [name]

- a photo of the small [name]
- a photo of the weird [name]
- a photo of the large [name]
- a photo of a cool [name]
- a photo of a small [name]
- a photo of a [name] playing sports
- a rendering of a [name] at a concert
- a cropped photo of the [name] cooking dinner
- the photo of a [name] at the beach
- a photo of a clean [name] participating in a marathon
- a photo of a dirty [name] after a mud run
- a dark photo of the [name] exploring a cave
- a photo of my [name] at graduation
- a photo of the cool [name] performing on stage
- a close-up photo of a [name] reading a book
- a bright photo of the [name] at a theme park
- a cropped photo of a [name] hiking in the mountains
- a photo of the [name] painting a mural
- a good photo of the [name] at a party
- a photo of one [name] playing an instrument
- a close-up photo of the [name] giving a speech
- a rendition of the [name] during a workout
- a photo of the clean [name] gardening
- a rendition of a [name] dancing in the rain
- a photo of a nice [name] volunteering at a charity event
- a photo of a [name] surfing a giant wave
- a rendering of a [name] skydiving over a scenic landscape
- a cropped photo of the [name] riding a rollercoaster
- the photo of a [name] rock climbing a steep cliff
- a photo of a clean [name] practicing yoga in a peaceful garden
- a photo of a dirty [name] participating in a paintball match
- a dark photo of the [name] stargazing at a remote location
- a photo of my [name] crossing the finish line at a race
- a photo of the cool [name] breakdancing in a crowded street
- a close-up photo of a [name] blowing out candles on a birthday cake
- a bright photo of the [name] flying a kite on a sunny day
- a cropped photo of a [name] ice-skating in a winter wonderland
- a photo of the [name] directing a short film
- a good photo of the [name] participating in a flash mob
- a photo of one [name] skateboarding in an urban park
- a close-up photo of the [name] solving a Rubik's cube
- a rendition of the [name] fire dancing at a beach party
- a photo of the clean [name] planting a tree in a com-

munity park

- a rendition of a [name] performing a magic trick on stage
  - a photo of a nice [name] rescuing a kitten from a tree
3. Prompts used during inference for multiple customized concepts attribution. The [name\_object] and [name\_style] placeholders are replaced by the specific watermarked tokens during the experiment.
- a photo of a [name\_object] in the style of [name\_style] with a clear background.
  - a rendering of a [name\_object] in the style of [name\_style] with a clear background.
  - a cropped photo of the [name\_object] in the style of [name\_style] with a clear background.
  - the photo of a [name\_object] in the style of [name\_style] with a clear background.
  - a photo of a clean [name\_object] in the style of [name\_style] with a clear background.
  - a photo of a dirty [name\_object] in the style of [name\_style] with a clear background.
  - a dark photo of the [name\_object] in the style of [name\_style] with a clear background.
  - a photo of my [name\_object] in the style of [name\_style] with a clear background.
  - a photo of the cool [name\_object] in the style of [name\_style] with a clear background.
  - a close-up photo of a [name\_object] in the style of [name\_style] with a clear background.
  - a bright photo of the [name\_object] in the style of [name\_style] with a clear background.
  - a cropped photo of a [name\_object] in the style of [name\_style] with a clear background.
  - a photo of the [name\_object] in the style of [name\_style] with a clear background.
  - a good photo of the [name\_object] in the style of [name\_style] with a clear background.
  - a photo of one [name\_object] in the style of [name\_style] with a clear background.
  - a close-up photo of the [name\_object] in the style of [name\_style] with a clear background.
  - a rendition of the [name\_object] in the style of [name\_style] with a clear background.
  - a photo of the clean [name\_object] in the style of [name\_style] with a clear background.
  - a rendition of a [name\_object] in the style of [name\_style] with a clear background.
  - a photo of a nice [name\_object] in the style of [name\_style] with a clear background.
  - a good photo of a [name\_object] in the style of [name\_style] with a clear background.
  - a photo of the nice [name\_object] in the style of [name\_style] with a clear background.
  - a photo of the small [name\_object] in the style of

[name\_style] with a clear background.

- a photo of the weird [name\_object] in the style of [name\_style] with a clear background.
- a photo of the large [name\_object] in the style of [name\_style] with a clear background.
- a photo of a cool [name\_object] in the style of [name\_style] with a clear background.
- a photo of a small [name\_object] in the style of [name\_style] with a clear background.

## References

- [1] Vishal Asnani, Xi Yin, Tal Hassner, Sijia Liu, and Xiaoming Liu. Proactive image manipulation detection. In *Proceedings of the IEEE/CVF conference on computer vision and pattern recognition*, pages 15386–15395, 2022. [2](#)
- [2] Vishal Asnani, John Collomosse, Tu Bui, Xiaoming Liu, and Shruti Agarwal. Promark: Proactive diffusion watermarking for causal attribution. In *Proceedings of the IEEE/CVF Conference on Computer Vision and Pattern Recognition*, pages 10802–10811, 2024. [1](#), [2](#), [5](#), [6](#)
- [3] Vishal Asnani, John Collomosse, Xiaoming Liu, and Shruti Agarwal. Custommark: Customization of diffusion models for proactive attribution. In *APAI workshop on International Conference on Computer Vision*, 2025. [1](#), [2](#), [5](#), [6](#), [7](#)
- [4] Muhammad Awais, Muzammal Naseer, Salman Khan, Rao Muhammad Anwer, Hisham Cholakkal, Mubarak Shah, Ming-Hsuan Yang, and Fahad Shahbaz Khan. Foundation models defining a new era in vision: a survey and outlook. *IEEE Transactions on Pattern Analysis and Machine Intelligence*, 2025. [1](#)
- [5] Kar Balan, Shruti Agarwal, Simon Jenni, Andy Parsons, Andrew Gilbert, and John Collomosse. Ekila: Synthetic media provenance and attribution for generative art. In *Proceedings of the IEEE/CVF Conference on Computer Vision and Pattern Recognition*, pages 913–922, 2023. [5](#), [6](#)
- [6] Tom Brown, Benjamin Mann, Nick Ryder, Melanie Subbiah, Jared D Kaplan, Prafulla Dhariwal, Arvind Neelakantan, Pranav Shyam, Girish Sastry, Amanda Askell, et al. Language models are few-shot learners. *Advances in neural information processing systems*, 33:1877–1901, 2020. [5](#), [7](#)
- [7] Anh Bui, Trang Vu, Trung Le, Junae Kim, Tamas Abraham, Rollin Omari, Amar Kaur, and Dinh Phung. Mitigating semantic collapse in generative personalization with a surprisingly simple test-time embedding adjustment. *arXiv preprint arXiv:2506.22685*, 2025. [2](#)
- [8] Xi Chen, Lianghua Huang, Yu Liu, Yujun Shen, Deli Zhao, and Hengshuang Zhao. Anydoor: Zero-shot object-level image customization. In *Proceedings of the IEEE/CVF conference on computer vision and pattern recognition*, pages 6593–6602, 2024. [2](#)
- [9] Simon Chesterman. Good models borrow, great models steal: intellectual property rights and generative ai. *Policy and Society*, 44(1):23–37, 2025. [2](#)
- [10] Jia Deng, Wei Dong, Richard Socher, Li-Jia Li, Kai Li, and Li Fei-Fei. Imagenet: A large-scale hierarchical image database. In *2009 IEEE conference on computer vision and pattern recognition*, pages 248–255. Ieee, 2009. [5](#), [6](#)

- [11] Patrick Esser, Sumith Kulal, Andreas Blattmann, Rahim Entezari, Jonas Müller, Harry Saini, Yam Levi, Dominik Lorenz, Axel Sauer, Frederic Boesel, et al. Scaling rectified flow transformers for high-resolution image synthesis. In *Forty-first international conference on machine learning*, 2024. 1
- [12] Weitao Feng, Jiyan He, Jie Zhang, Tianwei Zhang, Wenbo Zhou, Weiming Zhang, and Nenghai Yu. Catch you everything everywhere: Guarding textual inversion via concept watermarking. *arXiv preprint arXiv:2309.05940*, 2023. 2
- [13] Pierre Fernandez, Guillaume Couairon, Hervé Jégou, Matthijs Douze, and Teddy Furon. The stable signature: Rooting watermarks in latent diffusion models. In *Proceedings of the IEEE/CVF International Conference on Computer Vision*, pages 22466–22477, 2023. 1, 2
- [14] Rinon Gal, Yuval Alaluf, Yuval Atzmon, Or Patashnik, Amit H Bermano, Gal Chechik, and Daniel Cohen-Or. An image is worth one word: Personalizing text-to-image generation using textual inversion. *arXiv preprint arXiv:2208.01618*, 2022. 2
- [15] Emir Ganic and Ahmet M Eskicioglu. Robust dwt-svd domain image watermarking: embedding data in all frequencies. In *Proceedings of the 2004 Workshop on Multimedia and Security*, pages 166–174, 2004. 2
- [16] Martin Heusel, Hubert Ramsauer, Thomas Unterthiner, Bernhard Nessler, and Sepp Hochreiter. Gans trained by a two time-scale update rule converge to a local nash equilibrium. *Advances in neural information processing systems*, 30, 2017. 6
- [17] Neil Houlsby, Andrei Giurgiu, Stanislaw Jastrzebski, Bruna Morrone, Quentin De Laroussilhe, Andrea Gesmundo, Mona Attariyan, and Sylvain Gelly. Parameter-efficient transfer learning for nlp. In *International conference on machine learning*, pages 2790–2799. PMLR, 2019. 4
- [18] Huayang Huang, Yu Wu, and Qian Wang. Robin: Robust and invisible watermarks for diffusion models with adversarial optimization. *Advances in Neural Information Processing Systems*, 37:3937–3963, 2024. 2
- [19] Yi Huang, Jiancheng Huang, Yifan Liu, Mingfu Yan, Jiayi Lv, Jianzhuang Liu, Wei Xiong, He Zhang, Liangliang Cao, and Shifeng Chen. Diffusion model-based image editing: A survey. *IEEE Transactions on Pattern Analysis and Machine Intelligence*, 2025. 1
- [20] Menglin Jia, Luming Tang, Bor-Chun Chen, Claire Cardie, Serge Belongie, Bharath Hariharan, and Ser-Nam Lim. Visual prompt tuning. In *European conference on computer vision*, pages 709–727. Springer, 2022. 2
- [21] Chanwoo Kim, Soham U Gadgil, Alex J DeGrave, Jesu- ofunmi A Omiye, Zhuo Ran Cai, Roxana Daneshjou, and Su-In Lee. Transparent medical image ai via an image–text foundation model grounded in medical literature. *Nature medicine*, 30(4):1154–1165, 2024. 1
- [22] Nupur Kumari, Bingliang Zhang, Richard Zhang, Eli Shechtman, and Jun-Yan Zhu. Multi-concept customization of text-to-image diffusion. In *Proceedings of the IEEE/CVF conference on computer vision and pattern recognition*, pages 1931–1941, 2023. 2
- [23] Zhen Li, Mingdeng Cao, Xintao Wang, Zhongang Qi, Ming-Ming Cheng, and Ying Shan. Photomaker: Customizing realistic human photos via stacked id embedding. In *Proceedings of the IEEE/CVF conference on computer vision and pattern recognition*, pages 8640–8650, 2024. 2
- [24] Laurens van der Maaten and Geoffrey Hinton. Visualizing data using t-sne. *Journal of machine learning research*, 9 (Nov):2579–2605, 2008. 2
- [25] Andreas Müller, Denis Lukovnikov, Jonas Thietke, Asja Fischer, and Erwin Quiring. Black-box forgery attacks on semantic watermarks for diffusion models. In *Proceedings of the Computer Vision and Pattern Recognition Conference*, pages 20937–20946, 2025. 2
- [26] Hong-Hanh Nguyen-Le, Van-Tuan Tran, Thuc Nguyen, and Nhien-An Le-Khac. A survey on proactive deepfake defense: Disruption and watermarking. *ACM Computing Surveys*, 2025. 2
- [27] Ed Pizzi, Sreya Dutta Roy, Sugosh Nagavara Ravindra, Priya Goyal, and Matthijs Douze. A self-supervised descriptor for image copy detection. In *Proceedings of the IEEE/CVF Conference on Computer Vision and Pattern Recognition*, pages 14532–14542, 2022. 5, 6
- [28] Alec Radford, Jong Wook Kim, Chris Hallacy, Aditya Ramesh, Gabriel Goh, Sandhini Agarwal, Girish Sastry, Amanda Askell, Pamela Mishkin, Jack Clark, et al. Learning transferable visual models from natural language supervision. In *International conference on machine learning*, pages 8748–8763. PmLR, 2021. 3, 5, 6
- [29] Ahmad Rezaei, Mohammad Akbari, Saeed Ranjbar Alvar, Arezou Fatemi, and Yong Zhang. Lawa: Using latent space for in-generation image watermarking. In *European Conference on Computer Vision*, pages 118–136. Springer, 2024. 1
- [30] Robin Rombach, Andreas Blattmann, Dominik Lorenz, Patrick Esser, and Björn Ommer. High-resolution image synthesis with latent diffusion models. In *Proceedings of the IEEE/CVF conference on computer vision and pattern recognition*, pages 10684–10695, 2022. 1, 2, 5
- [31] Nataniel Ruiz, Yuanzhen Li, Varun Jampani, Yael Pritch, Michael Rubinstein, and Kfir Aberman. Dreambooth: Fine tuning text-to-image diffusion models for subject-driven generation. In *Proceedings of the IEEE/CVF conference on computer vision and pattern recognition*, pages 22500–22510, 2023. 1, 2
- [32] Dan Ruta, Saeid Motiian, Baldo Faieta, Zhe Lin, Hailin Jin, Alex Filipkowski, Andrew Gilbert, and John Collomosse. Aladin: All layer adaptive instance normalization for fine-grained style similarity. In *Proceedings of the IEEE/CVF International Conference on Computer Vision*, pages 11926–11935, 2021. 5, 6
- [33] Chitwan Saharia, William Chan, Saurabh Saxena, Lala Li, Jay Whang, Emily L Denton, Kamyar Ghasemipour, Raphael Gontijo Lopes, Burcu Karagol Ayan, Tim Salimans, et al. Photorealistic text-to-image diffusion models with deep language understanding. *Advances in neural information processing systems*, 35:36479–36494, 2022. 2
- [34] Tom Sander, Pierre Fernandez, Alain Durmus, Teddy Furon, and Matthijs Douze. Watermark anything with localized

- messages. In *International Conference on Learning Representations (ICLR)*, 2025. 1, 2
- [35] Amit Kumar Singh, Nomit Sharma, Mayank Dave, and Anand Mohan. A novel technique for digital image watermarking in spatial domain. In *2012 2nd IEEE International Conference on Parallel, Distributed and Grid Computing*, pages 497–501. IEEE, 2012. 2
- [36] Gowthami Somepalli, Anubhav Gupta, Kamal Gupta, Shramay Palta, Micah Goldblum, Jonas Geiping, Abhinav Shrivastava, and Tom Goldstein. Measuring style similarity in diffusion models. *arXiv preprint arXiv:2404.01292*, 2024. 4
- [37] Wei Ren Tan, Chee Seng Chan, Hernan E Aguirre, and Kiyoshi Tanaka. Improved artgan for conditional synthesis of natural image and artwork. *IEEE Transactions on Image Processing*, 28(1):394–409, 2018. 5
- [38] Saliltorn Thongmeensuk. Rethinking copyright exceptions in the era of generative ai: Balancing innovation and intellectual property protection. *The Journal of World Intellectual Property*, 27(2):278–295, 2024. 2
- [39] Kalpana Tyagi. Copyright, text & data mining and the innovation dimension of generative ai. *Journal of Intellectual Property Law & Practice*, 19(7):557–570, 2024. 2
- [40] Guanjie Wang, Zehua Ma, Chang Liu, Xi Yang, Han Fang, Weiming Zhang, and Nenghai Yu. Must: Robust image watermarking for multi-source tracing. In *Proceedings of the AAAI Conference on Artificial Intelligence*, pages 5364–5371, 2024. 1
- [41] Hanyi Wang, Han Fang, Shi-Lin Wang, and Ee-Chien Chang. Roar: Reducing inversion error in generative image watermarking. In *Proceedings of the IEEE/CVF International Conference on Computer Vision*, pages 19742–19751, 2025. 2
- [42] Run Wang, Felix Juefei-Xu, Meng Luo, Yang Liu, and Lina Wang. Faketagger: Robust safeguards against deepfake dissemination via provenance tracking. In *Proceedings of the 29th ACM international conference on multimedia*, pages 3546–3555, 2021. 2
- [43] Sheng-Yu Wang, Alexei A Efros, Jun-Yan Zhu, and Richard Zhang. Evaluating data attribution for text-to-image models. In *Proceedings of the IEEE/CVF International Conference on Computer Vision*, pages 7192–7203, 2023. 5, 6
- [44] Zhendong Wang, Jianmin Bao, Shuyang Gu, Dong Chen, Wengang Zhou, and Houqiang Li. Designdiffusion: High-quality text-to-design image generation with diffusion models. In *Proceedings of the Computer Vision and Pattern Recognition Conference*, pages 20906–20915, 2025. 2
- [45] Zilan Wang, Junfeng Guo, Jiacheng Zhu, Yiming Li, Heng Huang, Muhao Chen, and Zhengzhong Tu. Sleepermark: Towards robust watermark against fine-tuning text-to-image diffusion models. In *Proceedings of the Computer Vision and Pattern Recognition Conference*, pages 8213–8224, 2025. 1, 2
- [46] Yuxiang Wei, Yabo Zhang, Zhilong Ji, Jinfeng Bai, Lei Zhang, and Wangmeng Zuo. Elite: Encoding visual concepts into textual embeddings for customized text-to-image generation. In *Proceedings of the IEEE/CVF International Conference on Computer Vision*, pages 15943–15953, 2023. 2
- [47] Zijin Yang, Kai Zeng, Kejiang Chen, Han Fang, Weiming Zhang, and Nenghai Yu. Gaussian shading: Provable performance-lossless image watermarking for diffusion models. In *Proceedings of the IEEE/CVF Conference on Computer Vision and Pattern Recognition*, pages 12162–12171, 2024. 2
- [48] Gong Zhang, Kai Wang, Xingqian Xu, Zhangyang Wang, and Humphrey Shi. Forget-me-not: Learning to forget in text-to-image diffusion models. In *Proceedings of the IEEE/CVF conference on computer vision and pattern recognition*, pages 1755–1764, 2024. 2
- [49] Xuanyu Zhang, Zecheng Tang, Zhipei Xu, Runyi Li, Youmin Xu, Bin Chen, Feng Gao, and Jian Zhang. Omniguard: Hybrid manipulation localization via augmented versatile deep image watermarking. In *Proceedings of the Computer Vision and Pattern Recognition Conference*, pages 3008–3018, 2025. 2
- [50] Yuxuan Zhang, Yirui Yuan, Yiren Song, Haofan Wang, and Jiaming Liu. Easycontrol: Adding efficient and flexible control for diffusion transformer. In *Proceedings of the IEEE/CVF International Conference on Computer Vision*, pages 19513–19524, 2025. 2
- [51] Xuandong Zhao, Kexun Zhang, Zihao Su, Saastha Vasani, Ilya Grishchenko, Christopher Kruegel, Giovanni Vigna, Yuxiang Wang, and Lei Li. Invisible image watermarks are provably removable using generative ai. *Advances in neural information processing systems*, 37:8643–8672, 2024. 8
- [52] Yuan Zhao, Bo Liu, Ming Ding, Baoping Liu, Tianqing Zhu, and Xin Yu. Proactive deepfake defence via identity watermarking. In *Proceedings of the IEEE/CVF winter conference on applications of computer vision*, pages 4602–4611, 2023. 2
- [53] Kaiyang Zhou, Jingkang Yang, Chen Change Loy, and Ziwei Liu. Conditional prompt learning for vision-language models. In *Proceedings of the IEEE/CVF conference on computer vision and pattern recognition*, pages 16816–16825, 2022. 2
- [54] Jiren Zhu, Russell Kaplan, Justin Johnson, and Li Fei-Fei. Hidden: Hiding data with deep networks. In *Proceedings of the European conference on computer vision (ECCV)*, pages 657–672, 2018. 2
- [55] Peifei Zhu, Tsubasa Takahashi, and Hirokatsu Kataoka. Watermark-embedded adversarial examples for copyright protection against diffusion models. In *Proceedings of the IEEE/CVF Conference on Computer Vision and Pattern Recognition*, pages 24420–24430, 2024. 1